

Supporting Information

High-valence chromium accelerated interface electron transfer for water oxidation

Shaoxi Kong,^{a†} Mengfei Lu,^{a,b†} Shicheng Yan,^{a*} and Zhigang Zou^{a,b}

^aCollaborative Innovation Center of Advanced Microstructures, Eco-materials and Renewable Energy Research Center (ERERC), College of Engineering and Applied Sciences, Nanjing University, No. 22, Hankou Road, Nanjing, Jiangsu 210093, P. R. China.

^bNational Laboratory of Solid State Microstructures, Jiangsu Key Laboratory for Nano Technology, School of Physics, Nanjing University, No. 22 Hankou Road, Nanjing, Jiangsu 210093, P. R. China.

* Corresponding Author E-mail: yscfei@nju.edu.cn (S. C. Yan)

† These authors contributed equally to this work.

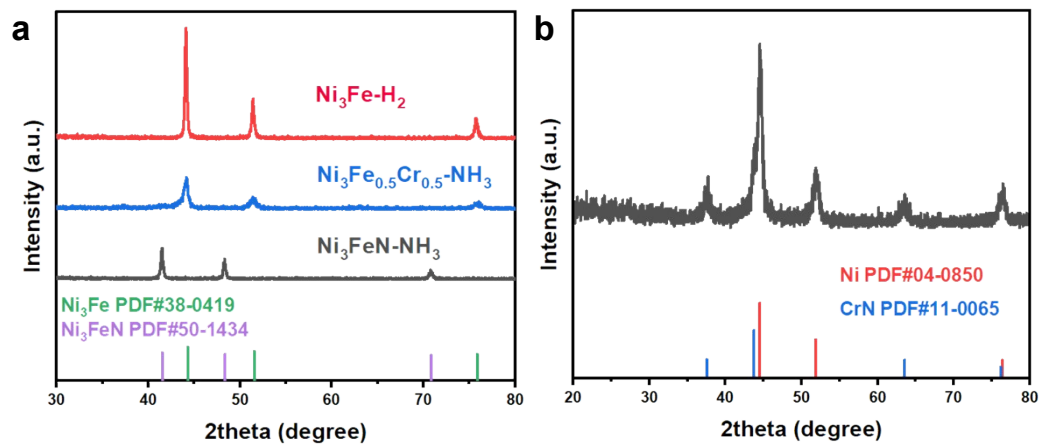


Fig S1. (a) XRD patterns of $\text{Ni}_3\text{Fe}_{0.5}\text{Cr}_{0.5}\text{-NH}_3$, $\text{Ni}_3\text{Fe-H}_2$ and $\text{Ni}_3\text{FeN-NH}_3$. (b) XRD pattern of $\text{Ni}_3\text{Cr-NH}_3$.

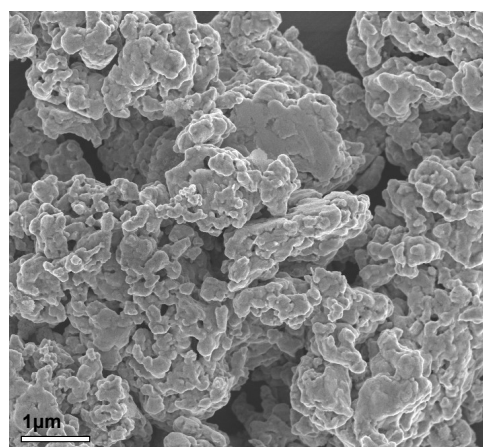


Fig S2. SEM image of Ni₃Fe.

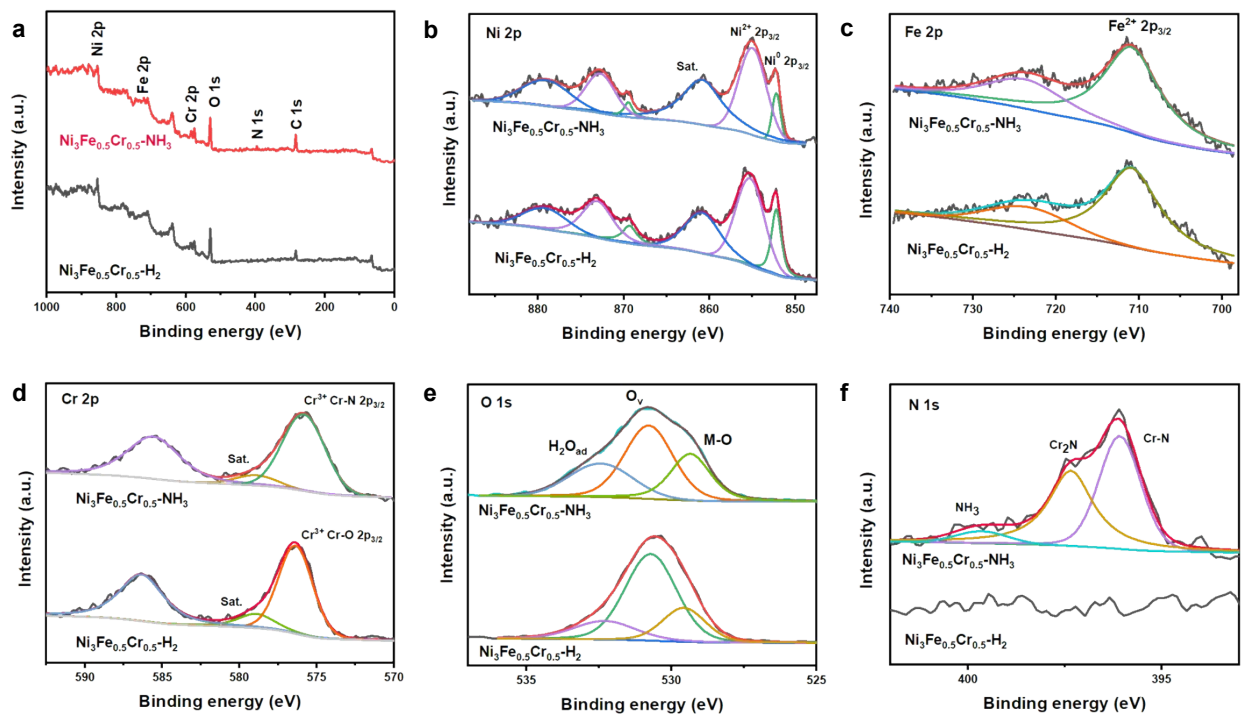


Fig S3. XPS spectra. (a) Survey spectra, (b) Ni 2p, (c) Fe 2p, (d) Cr 2p, (e) O 1s and (f) N 1s for $\text{Ni}_3\text{Fe}_{0.5}\text{Cr}_{0.5}-\text{NH}_3$ and $\text{Ni}_3\text{Fe}_{0.5}\text{Cr}_{0.5}-\text{H}_2$.

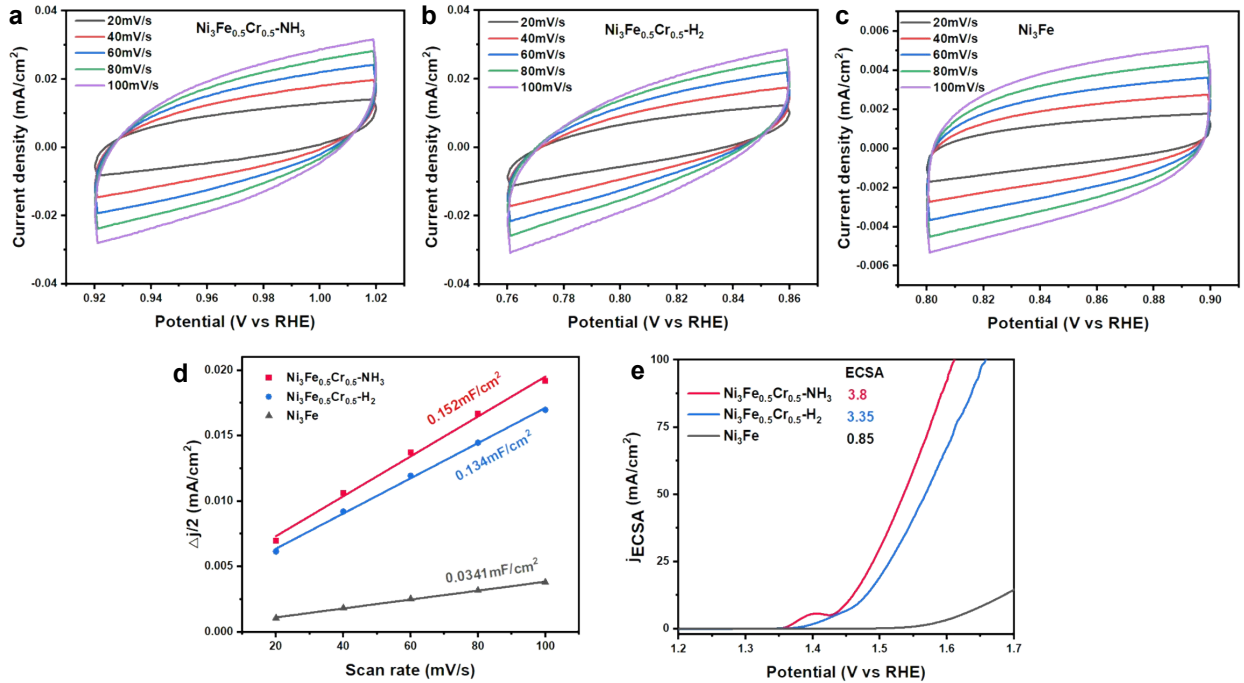


Fig S4. CV curves with different scan rates in non-faradic region. (a) $\text{Ni}_3\text{Fe}_{0.5}\text{Cr}_{0.5}\text{-NH}_3$, (b) $\text{Ni}_3\text{Fe}_{0.5}\text{Cr}_{0.5}\text{-H}_2$, (c) Ni_3Fe at various scan rates (20, 40, 60, 80 and 100 mV/s) in 1.0 M KOH for OER. (d) Plots of capacitive current density versus scan rate. The slopes represent C_{dl} . (e) LSV curves normalized by ECSA of the as-prepared samples. The ECSA was calculated by double-layer capacitance.

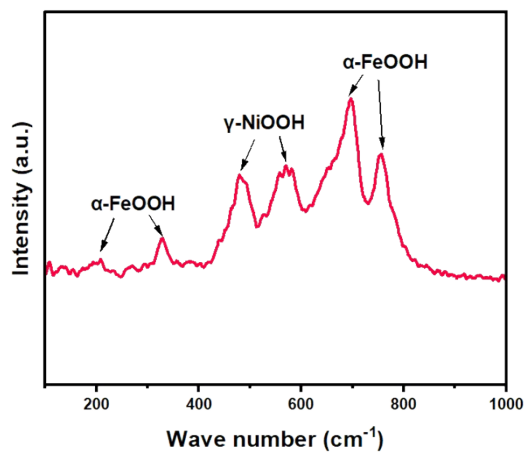


Fig S5. Raman spectrum of $\text{Ni}_3\text{Fe}_{0.5}\text{Cr}_{0.5}\text{-NH}_3$ after OER.

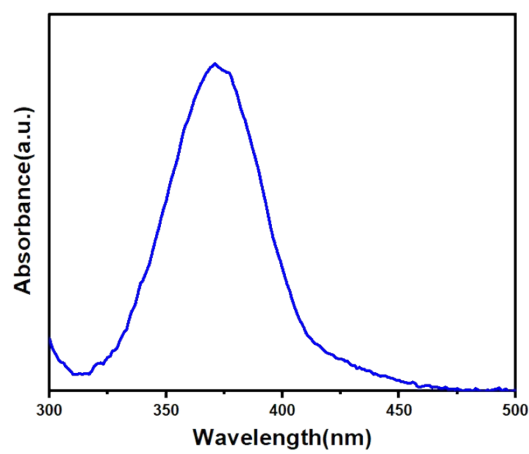


Fig S6. UV-vis spectroscopy of the electrolyte after the chronoamperometry measurement.

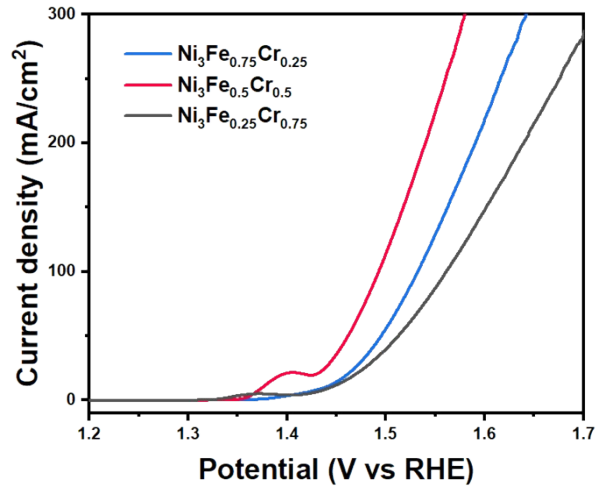


Fig S7.OER polarization curves of $\text{Ni}_3\text{Fe}_{1-x}\text{Cr}_x-\text{NH}_3$ ($x=0.25, 0.5, 0.75$) with 90 % iR correction at a scan rate of 10 mV/s in 1.0 M KOH.

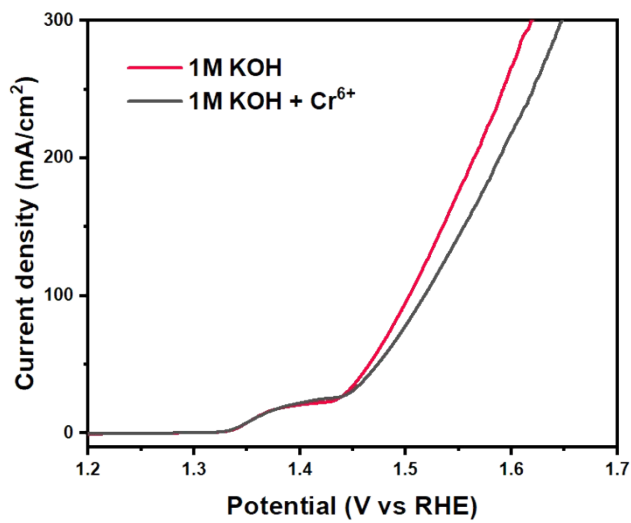


Fig S8. OER polarization curves of $\text{Ni}_3\text{Fe}_{0.5}\text{Cr}_{0.5}-\text{NH}_3$ with 90 % iR correction at a scan rate of 10 mV/s in 1.0 M KOH and 1.0 M KOH with Cr^{6+} .

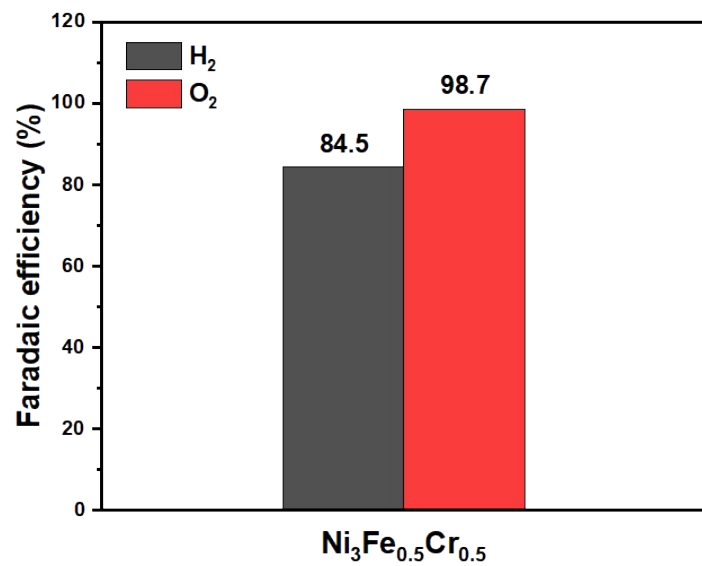


Fig S9. The faradaic efficiency of $\text{Ni}_3\text{Fe}_{0.5}\text{Cr}_{0.5}-\text{NH}_3$.

Table S1. Compositions of the samples determined by ICP-AES.

Samples	The content of metal ions (mmol/L)			Mole ratio		
	Ni	Fe	Cr	Ni	Fe	Cr
$\text{Ni}_3\text{Fe}_{0.5}\text{Cr}_{0.5}$	1.20	0.21	0.18	3.08	0.54	0.46
After 10h OER	0.2835	0.0500	0.0047	3.06	0.54	0.051
After 20h OER	0.1894	0.0340	0.0033	2.99	0.54	0.05

Table S2. Concentrations of Cr Fe and Ni for $\text{Ni}_3\text{Fe}_{0.5}\text{Cr}_{0.5}\text{-NH}_3$ after operating in different electrolytes, as shown in **Fig 5b**, determined by the atomic absorption spectrum.

	0-10h OER	10-20h OER
Concentration of Cr(μg/L)	237.66	ND
Concentration of Fe(μg/L)	ND	ND
Concentration of Ni(μg/L)	ND	ND

Table S3. Comparison of the OER performance of $\text{Ni}_3\text{Fe}_{0.5}\text{Cr}_{0.5}\text{-NH}_3$ to the recently reported Cr-NiFe catalysts.

Catalyst	Electrolyte	Substrates	Method	j (mA cm ⁻²)	η (mV)	Reference
$\text{Ni}_3\text{Fe}_{0.5}\text{Cr}_{0.5}\text{-NH}_3$	1.0 M KOH	Carbon paper	Dropping	25 50	209 232	This work
NiFeCr-LDH	1.0 M KOH	Ni foam	Dropping	100	242	[1]
NiFeCr-LDH/MoS ₂	1.0 M KOH	glassy carbon	Dropping	10	270	[2]
NiFeCr LDH	1.0 M KOH	Carbon paper	In situ growth	25	225	[3]
h-NiFeCr	1.0 M KOH	Ni foam	Electrodeposition	10	220	[4]
NiFeCr	1.0 M KOH	Ni foam	Electrodeposition	100	260	[5]
Cr ₁ /FeNi-LDH	1.0 M KOH	stainless steel	Electrodeposition	10	202	[6]
CS-NiFeCr	1.0 M KOH	Copper foil	Electrodeposition	10 50	200 230	[7]

References

1. Wang, M. H.; Lou, Z. X.; Wu, X.; Liu, Y.; Zhao, J. Y.; Sun, K. Z.; Li, W. X.; Chen, J.; Yuan, H. Y.; Zhu, M.; Dai, S.; Liu, P. F.; Yang, H. G., *Small* **2022**, *18*, e2200303.
2. Chen, S.; Yu, C.; Cao, Z.; Huang, X.; Wang, S.; Zhong, H., *Int. J. Hydr. Energy* **2021**, *46*, 7037-7046.
3. Yang, Y.; Dang, L.; Shearer, M. J.; Sheng, H.; Li, W.; Chen, J.; Xiao, P.; Zhang, Y.; Hamers, R. J.; Jin, S., *Adv. Energy Mater* **2018**, *8*, 1703189.
4. Bo, X.; Li, Y.; Hocking, R. K.; Zhao, C., *ACS Appl Mater Interfaces* **2017**, *9*, 41239-41245.
5. Bo, X.; Hocking, R. K.; Zhou, S.; Li, Y.; Chen, X.; Zhuang, J.; Du, Y.; Zhao, C., *Energy Environ. Sci* **2020**, *13*, 4225-4237.
6. Xie, X.; Cao, C.; Wei, W.; Zhou, S.; Wu, X. T.; Zhu, Q. L., *Nanoscale* **2020**, *12*, 5817-5823.
7. Fan, L.; Zhang, P.; Zhang, B.; Daniel, Q.; Timmer, B. J. J.; Zhang, F.; Sun, L. *ACS Energy Lett* **2018**, *3*, 2865-2874.